Design and Fabrication of a Microstrip Low-Pass Filter with a Wide Stopband Using a Windmill-Shaped Resonator

Sobhan Roshani[1], Salah I. Yahya[2,3], Shahram Khazaei[4], Saeed Roshani[1†], and Babak Karami[5]

[1]Department of Electrical Engineering, Kermanshah Branch, Islamic Azad University, Kermanshah, Iran

[2]Department of Communication and Computer Engineering, Cihan University-Erbil, Erbil, Iraq

[3]Department of Software Engineering, Faculty of Engineering, Koya University, Koya, Iraq

[4]Department of Electrical Engineering, Sanandaj Branch, Islamic Azad University, Sanandaj, Iran

[5]Department of Mechanical Engineering, Kermanshah Branch, Islamic Azad University, Kermanshah, Iran

***Abstract*—In this paper, a microstrip low-pass filter (LPF) with a wide stopband and a sharp transition band is presented using a windmill-shaped resonator. Traditional LPF designs often face challenges such as narrow stopbands, high insertion loss, and large physical sizes, which limit their performance in modern communication systems. To address these challenges, the proposed filter exhibits low insertion loss, a sharp response in the transition band, a wide stopband, and a compact size. The windmill-shaped resonator is applied to achieve a sharp response in the transition band, while two suppressor cells are added to extend the stopband. The filter has a 3 dB cutoff frequency (fc) of 1.61 GHz, with an S_{12} parameter value of −20 dB at 1.7 GHz, resulting in a narrow transition band of 0.18 GHz, demonstrating its superior performance. In addition, the filter achieves a wide stopband that extends from 1.79 GHz to 11.26 GHz (a bandwidth of 9.47 GHz) with high attenuation. The physical size of the filter is 13.34 mm × 12.78 mm (0.097λ × 0.093λ). Overall, the proposed filter demonstrates excellent characteristics in both the passband and stopband regions, providing an effective solution for modern communication system requirements. The presented design effectively addresses key limitations in traditional LPF configurations, offering improved performance and compactness.**

***Index Terms*—Low-pass filter, Microstrip, Resonator, Return loss, Stopband, Transition band.**

ARO-The Scientific Journal of Koya University
Vol. XII, No. 2 (2024), Article ID: ARO.11752. 8 pages
DOI: 10.14500/aro.11752
Received: 06 August 2024; Accepted: 17 November 2024
Regular research paper; Published: 01 December 2024
†Corresponding author's e-mail: s_roshani@iau.ir

I. Introduction

Microstrip low-pass filters (LPF) play a crucial role in modern microwave communication systems. To meet demands such as high performance and compact size, LPF with low power loss and wide stopbands are in high demand. Planar structures are highly advantageous in the design of LPF due to their simple geometry, which facilitates ease of fabrication and optimization. These structures offer a compact size, making them suitable for modern communication systems where space is a critical factor. In addition, planar designs are versatile and can be easily integrated with other components on a single substrate, enhancing overall system performance. Their ability to achieve sharp transition bands and wide stopbands while maintaining low insertion loss and good return loss further underscores their significance in LPF design. One of the most interesting techniques for microstrip filters is their structure, which employs a photonic bandgap (PBG) structure with a microstrip transmission line. The PBG structure exhibits slow-wave characteristics near the stopband in the passband region (Meade et al., 1991). In (Deng, Xue and Che, 2007), a LPF with a suitable wide stopband is presented, but the attenuation of unwanted signals in the stopband is insufficient. In (Li, Li and Wei, 2009), cone resonators are used to achieve a wide bandwidth, resulting in strong attenuation near the passband, which is an advantage, but the low sharpness of the filter's response is a drawback. In (Ting, Tam and Martins, 2006), a combination of DGS and dual U-shaped resonators are used to achieve high attenuation, but the return loss in the passband for this LPF is not acceptable. In (Luo, Zhu and Sun, 2008), another structure based on a coupled hairpin resonator is proposed, which has very small dimensions and performed well in the stopband and passband, but this structure also

suffered from gradual attenuation in the transition band. In (Mandal et al., 2006), a filter composed of complementary split-ring resonators is employed, which has a good return loss in the passband but not a very wide stopband. In (Park, Kim and Nam, 2007), a LPF with excellent performance is proposed, which utilizes parallel open stubs and a DGS structure simultaneously, achieving notable performance but having large dimensions. In (Yang et al., 2010), various types of DGS were also used for implementing LPF, including ring structures and stepped impedance, to achieve smaller dimensions while maintaining acceptable response performance. In (Ma and Yeo, 2010), a filter with a very wide stopband was achieved using modified radial resonators, but the structure is complex and has large physical dimensions. In (Roshani, Dehghani and Roshani, 2019), fountain-shaped resonators are used to create a compact LPF with a size of $0.135\lambda_g \times 0.132\lambda_g$. This LPF provides a wide stopband and sharp response but has complex structures. Resonators are also used to shape other types of microwave devices, such as dividers (Roshani et al., 2023b, Mohammadi et al., 2024), couplers (Hosseini and Rezaei, 2020), diplexers (Rezaei and Yahya, 2022), antenna arrays (Roshani et al., 2023a).

In (Wang et al., 2010), a LPF is reported with a cutoff frequency (fc) of 1.18 GHz. The relative stop bandwidth (RSB) of this filter is 1.32. Despite its reasonable performance in terms of cutoff frequency and sharpness, the size of this filter is large, and its frequency response is not as sharp as desired, making it less efficient for applications requiring compactness and high precision. In (Ma, Yeo and Lim, 2012), a microstrip LPF is reported with a 3.2 GHz cutoff frequency. This filter has a RSB of 1.66. The sharpness of this LPF is low and has a large size, making it less desirable for applications where space and precision are critical. In (Ge, Wang and Guo, 2010), a LPF is reported with a 1.3 GHz cutoff frequency and 37dB/GHz sharpness. This filter has a large size. The bulky design and lack of sharp frequency discrimination limit its suitability for compact and precise applications.

In (Challal et al., 2012), a LPF is reported with a 25 dB/GHz sharpness and 2.95 GHz cutoff frequency. This filter has a good response but occupies a large size. The large size and its gradual frequency response are significant drawbacks, which are not desirable.

In (Faraghi, Azarmanesh and Ojaroudi, 2013), a LPF is reported with a 3.4 GHz cutoff frequency. The filter features a RSB of 1.4 and a sharpness (ζ) of 37 dB/GHz. The overall size of the filter is large, and the frequency response is not sharp enough. These limitations make it less ideal for use modern communication systems. Moreover, recently, the open stub technique has gained significant attention in the design of LPFs due to its effectiveness in enhancing filter performance. This method provides a simple approach for achieving an improved suppression of unwanted harmonics. Incorporating open stubs into microstrip filters has proven beneficial in minimizing insertion loss while extending the stopband, making it a suitable option for advanced filter designs (Lotfi, Roshani and Roshani, 2020, Bavandpour et al., 2021, Chakraborty and Verma, 2024).

The novelty of the proposed microstrip LPF lies in its innovative use of a windmill-shaped resonator combined with asymmetrical suppressor cells, which together address several challenges present in conventional LPF designs. Traditional filters often face limitations such as narrow stopbands, high insertion loss, and large physical size. By integrating a compact windmill-shaped resonator, the proposed LPF achieves a sharp transition band and a significantly wider stopband while maintaining low insertion loss. In addition, the design's simplicity enhances manufacturability and allows for easy integration into modern communication circuits. These unique design features distinguish the proposed LPF, offering a compact and efficient solution that overcomes key limitations of prior LPF configurations.

The proposed LPF has potential applications across various modern communication systems where high performance, compactness, and efficiency are crucial. Its compact size and wide stopband make it ideal for integration into wireless communication devices, including mobile phones, Wi-Fi systems, and satellite communication equipment. The filter's low insertion loss and sharp transition band are particularly beneficial in frequency-selective environments, where efficient signal transmission and interference suppression are essential. In addition, the filter's wide stopband enhances its utility in multi-band and ultra-wideband applications by effectively attenuating out-of-band signals and preventing harmonic distortions. Given these characteristics, the proposed LPF can play a vital role in improving signal quality and minimizing interference in advanced communication infrastructure, including 5G networks, radar systems, and Internet of Things devices.

In this paper, a windmill-shaped resonator and two microstrip suppressing cells are used to design a LPF. The proposed structure has been simulated, fabricated, and measured. The proposed LPF has a simple planar structure, compact size, low insertion loss in the passband, and provides a wide stop band.

II. Design of the Proposed Resonator

The design process of the proposed filter consists of two stages. The first stage involves designing a windmill-shaped resonator to achieve a sharp response in the passband. The second stage entails designing an attenuator and adding it to the proposed resonator to achieve a wide stopband bandwidth.

A. Proposed Resonator

Fig. 1 shows the structure of the proposed resonator, which is formed by conical microstrip shapes arranged in the form of a windmill. The proposed structure has been simulated using the ADS simulator to provide the characteristics in both the passband and stopband.

The simulation results of the proposed resonator are shown in Fig. 2. The S_{12} curve is depicted with the blue line and the S11 curve is shown with red color. The results show that the cut-off frequency (fc) resonator is 1.4 GHz and

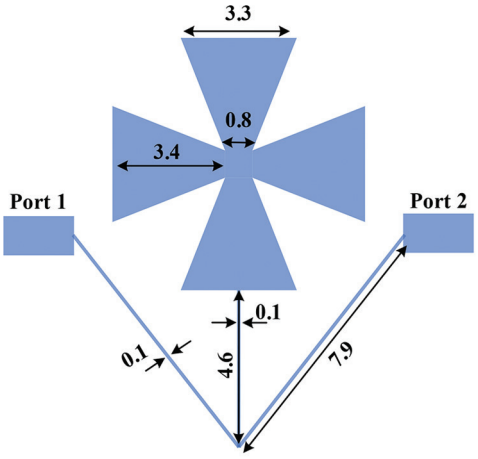

Fig. 1. Layout of the proposed resonator with conical microstrip shapes. All dimensions are written in millimeter.

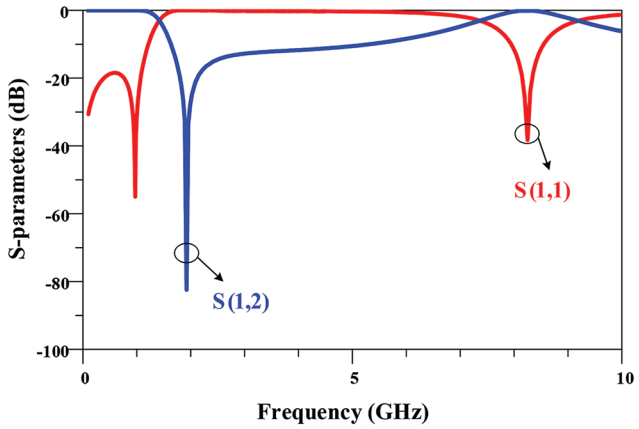

Fig. 2. Simulated Scattering parameter results of the proposed resonator.

provides transmission zero at 1.92 GHz with more than 80dB attenuation.

The equivalent LC circuit of the proposed resonator is shown in Fig. 3. In this equivalent circuit, L_2 represents the inductance of the transmission lines between the input and output ports. L_1 is the inductance of the transmission line connected to the resonator. C_1 is an open stub, representing the capacitance related to the conical resonator. EM simulated Scattering parameters of the proposed resonator and the equivalent LC circuit Simulation are depicted in Fig. 4, which have good agreements.

B. Proposed Suppressing Cells

The proposed resonator has suitable return loss, insertion loss, and sharpness of response. However, its stopband bandwidth is inadequate. Therefore, to improve the stopband bandwidth of the desired filter, as well as to enhance the sharpness of the response and the return loss, and considering the importance of simplicity in the filter structure, two asymmetrical stubs are used as suppressing cells. These open stubs create attenuation poles to suppress harmonics, resulting in significant attenuation at higher frequencies and providing a very wide stopband bandwidth. The structure of the suppressing cells is depicted in Fig. 5.

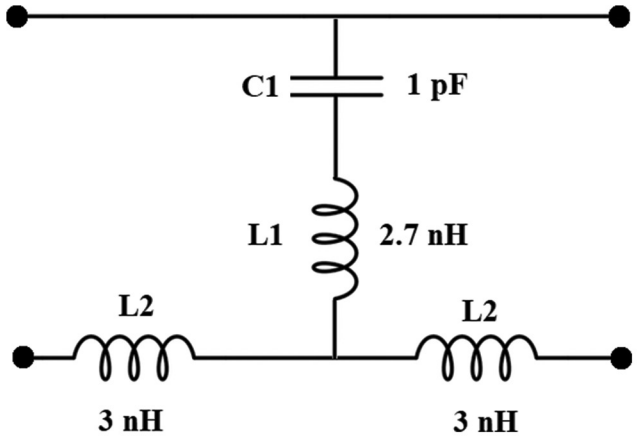

Fig. 3. Equivalent LC circuit of the proposed resonator.

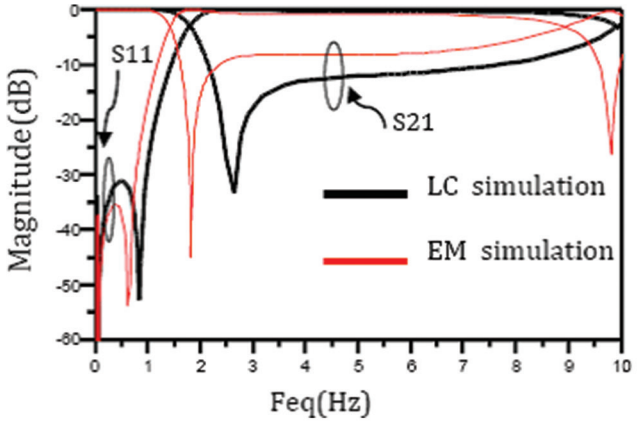

Fig. 4. EM simulated Scattering parameters the proposed resonator and the equivalent LC circuit Simulation.

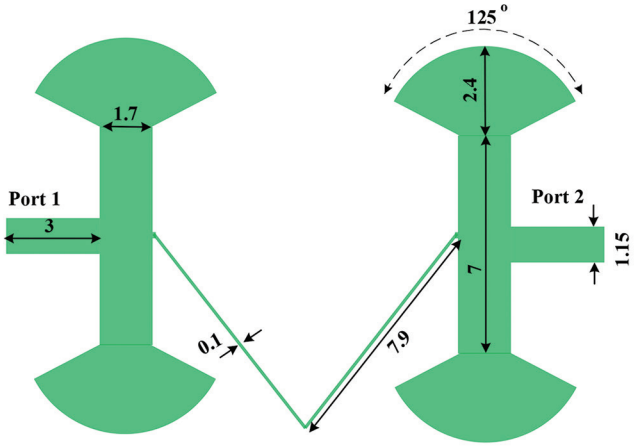

Fig. 5. Structure of the proposed suppressing cells. All dimensions are written in millimeter.

The simulated Scattering parameter results of the proposed suppressing cells are demonstrated in Fig. 6. The S_{12} curve is depicted with a blue line and the S11 curve is shown with red color. The results show that the cut-off frequency (fc) proposed suppressing cells is 1.42 GHz and provides two transmission zeros at 6.5 GHz and 7.5 GHz.

http://dx.doi.org/10.14500/aro.11752

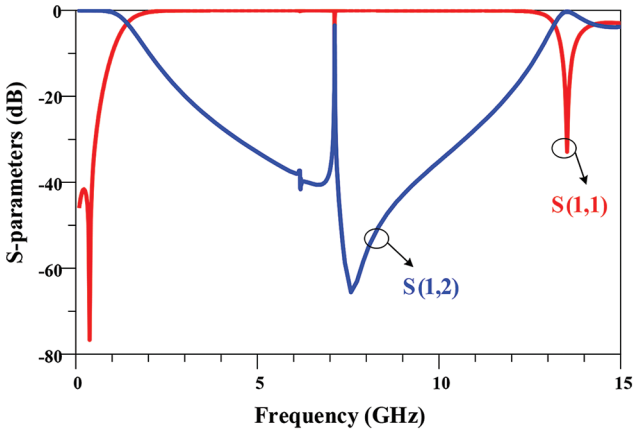

Fig. 6. Simulated Scattering parameter results of the proposed suppressing cells.

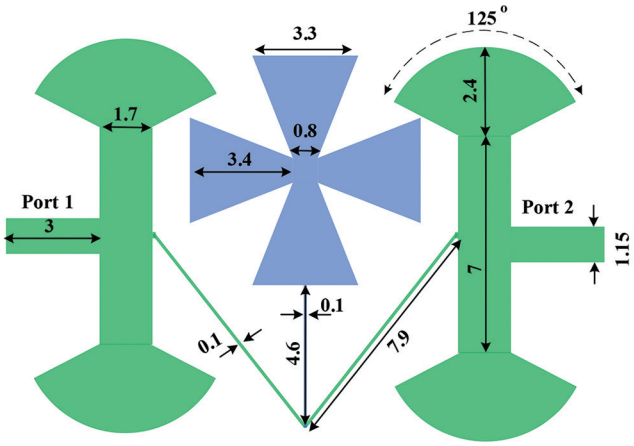

Fig. 7. Structure of the proposed low-pass filter. All dimensions are written in millimeter.

III. Design of the Proposed Filter

The proposed structure is designed based on the RT/Duroid 5880 with a dielectric constant of 2.2, a height of 15 mils, and a loss tangent of 0.0009. The layout of the proposed LPF is depicted in Fig. 7. For impedance matching, at the input and output ports with 50-ohm connectors, two microstrip lines are used.

Fig. 8 shows the simulated results of the designed filter. This filter has a 3 dB cutoff frequency of 1.61 GHz. This filter has a 3 dB cutoff frequency (fc) of 1.61 GHz. The value of the S_{12} parameter at a frequency of 1.7 GHz is -20 dB, resulting in a narrow transition band of 0.18 GHz, which demonstrates the acceptable performance of the proposed filter. The filter provides a wide stopband and has high attenuation in the stopband. The stopband extends from 1.79 GHz to 11.26 GHz (bandwidth of 9.47 GHz). The return loss in the passband is −16.64 dB, indicating the filter's good ability to pass power from port 1 to port 2. The insertion loss in the passband from DC to 1.5 GHz, which is approximately 95% of the passband, is 0.1 dB. Two transmission zeros are located at 1.89 GHz and 11.2 GHz with −55.53 dB and −42.22 dB, values, respectively. The physical size of the filter is only 13.34 mm × 12.78 mm (0.097λ × 0.093λ). Overall, it can be claimed that the proposed filter has good characteristics in both the passband and stopband regions.

The proposed LPF incorporates a windmill-shaped resonator and symmetrical suppressor cells, each playing a distinct role in achieving the filter's overall performance. The windmill-shaped resonator serves as the core structure, designed to achieve a sharp cutoff and precise control over the passband and transition band frequencies. This unique resonator shape leverages conical microstrip geometries to create a compact and effective configuration, enabling high-frequency selectivity and a narrow transition band. The windmill shape not only optimizes space but also ensures that the resonator operates effectively within a compact footprint, which is essential for applications requiring minimal size.

To further enhance the stopband characteristics, suppressor cells are incorporated. These suppressor cells are strategically positioned to create transmission zeros at specific frequencies within the stopband, effectively broadening the stopband

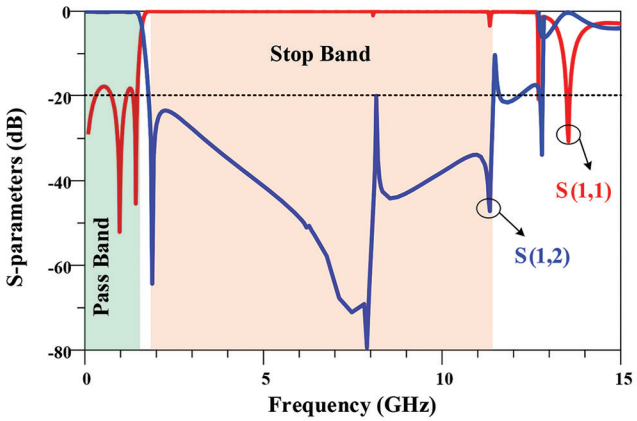

Fig. 8. Simulated and measured results of the designed Filter.

and ensuring strong attenuation of unwanted harmonics and interference. Suppressing cells introduces additional attenuation poles, which help maintain a high level of suppression across a wider frequency range, extending from 1.79 GHz to 11.26 GHz. This approach provides substantial interference reduction and minimizes signal leakage at frequencies above the passband. In addition, the LPF includes input and output matching networks formed by microstrip lines, which ensure impedance matching to 50 ohms, minimizing reflection losses at the interface with external circuitry. The filter is designed on an RT/Duroid 5880 substrate, chosen for its low dielectric loss and stable performance across high frequencies, further supporting low insertion loss and reliable performance.

Fig. 9 presents the surface current density distributions for the designed LPF at three different frequencies of 1.4 GHz, 7.7 GHz, and 12.2 GHz. At 1.4 GHz, which is located within the pass band, the surface current density is distributed such that the signal efficiently travels from the input to the output port. This indicates that the filter allows the desired frequency to pass through with minimal attenuation. Conversely, at 7.7 GHz and 12.2 GHz, both of which fall within the stop band, the surface current density plots demonstrate a significant reduction in current reaching port 2. This reduction signifies

the filter's capability to attenuate higher frequencies, effectively preventing them from propagating through to the output. The comparison across these frequencies highlights the filter's role in discriminating between the passband and stopband frequencies, ensuring that only frequencies below the cutoff of 1.61 GHz are transmitted, while higher frequencies are blocked.

IV. Ann model for the proposed LPF

The ANN model used in this study is designed to predict the scattering parameters of the proposed LPF, providing a data-driven approach to understanding the filter's behavior. The model architecture comprises three hidden layers with 20, 15, and 15 neurons, respectively, each optimized to capture the complex, non-linear relationships between input parameters and the LPF's performance characteristics. The proposed neural network architecture is illustrated in Fig. 10. The multi-layer perceptron (MLP) network is used to model and predict the scattering parameters. The MLP architecture consists of an input layer, three hidden layers, and an output layer corresponding to the predicted S-parameters. The network was optimized using a backpropagation algorithm and mean squared error as the loss function to minimize prediction errors. In the applied neural network, the Levenberg-Marquardt algorithm is used for backpropagation.

Real and predicted values for S_{11} and S_{21} parameters in train and test procedures are depicted in Fig. 11. As seen the data is predicted perfectly in both train and test procedures.

The real and predicted S-parameters for the proposed device model are depicted in Fig. 12. The proposed model has achieved high accuracy results in test and train mode. The results of the proposed ANN model show the MRE of 0.5018 and 0.1410 for the train and test phases of the S_{21} parameter. Furthermore, the MRE of 0.1331 and 0.2071 for the train and test phases of the S_{11} parameter are achieved.

V. Fabricated and Measured Results

The proposed structure is fabricated on RT/Duroid 5880 with a dielectric constant of 2.2, a height of 15 mils, and a loss tangent of 0.0009. The fabricated device is depicted in Fig. 13.

While the proposed LPF demonstrates excellent performance in terms of stopband bandwidth, insertion loss, and compact size, there are a few limitations in its design parameters. One notable constraint is the sensitivity of the filter's performance to variations in substrate material and manufacturing tolerances. The filter was fabricated on an RT/Duroid 5880 substrate, which, while effective, is relatively costly and may not be feasible for all applications, especially those requiring large-scale production. In addition, the high precision required for the windmill-shaped resonator and symmetrical suppressor cells makes the device susceptible to fabrication-induced variations, which can slightly affect the cutoff frequency and stopband characteristics if manufacturing tolerances are not strictly maintained. Moreover, while the filter achieves a sharp transition band and wide stopband, it is optimized for frequencies up to 11.26 GHz, limiting its applicability in systems requiring even higher frequency performance. The design's compactness also imposes some limitations on heat dissipation, which may impact performance in high-power applications. Despite these constraints, the proposed design remains highly effective within its intended operational range and offers a balanced solution for modern, compact communication systems. Further optimizations in materials and fabrication techniques could help mitigate these limitations and expand the filter's applicability.

Fig. 14 presents the measured and simulated S-parameters (S_{11} and S_{21}) of the designed LPF. The filter has a 3 dB cutoff frequency at 1.61 GHz, demonstrating its efficacy in passing frequencies below this threshold. Notably, the filter provides a wide stopband ranging from 1.79 GHz to 11.26 GHz, corresponding to a bandwidth of 9.47 GHz, and exhibits high

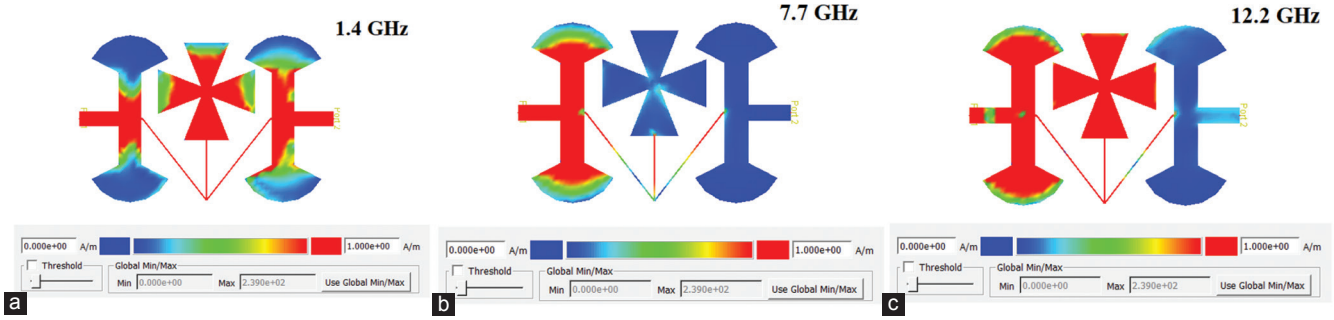

Fig. 9. Surface current density plots of the designed low-pass filter at three different frequencies: (a) 1.4 GHz (within the pass band), (b) 7.7 GHz (within the stop band), and (c) 12.2 GHz (within the stop band).

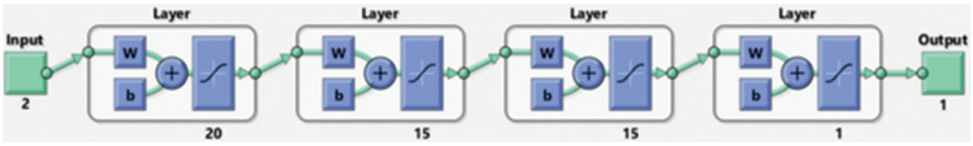

Fig. 10. Proposed neural network architecture of the designed low-pass filter with three hidden layers.

http://dx.doi.org/10.14500/aro.11752

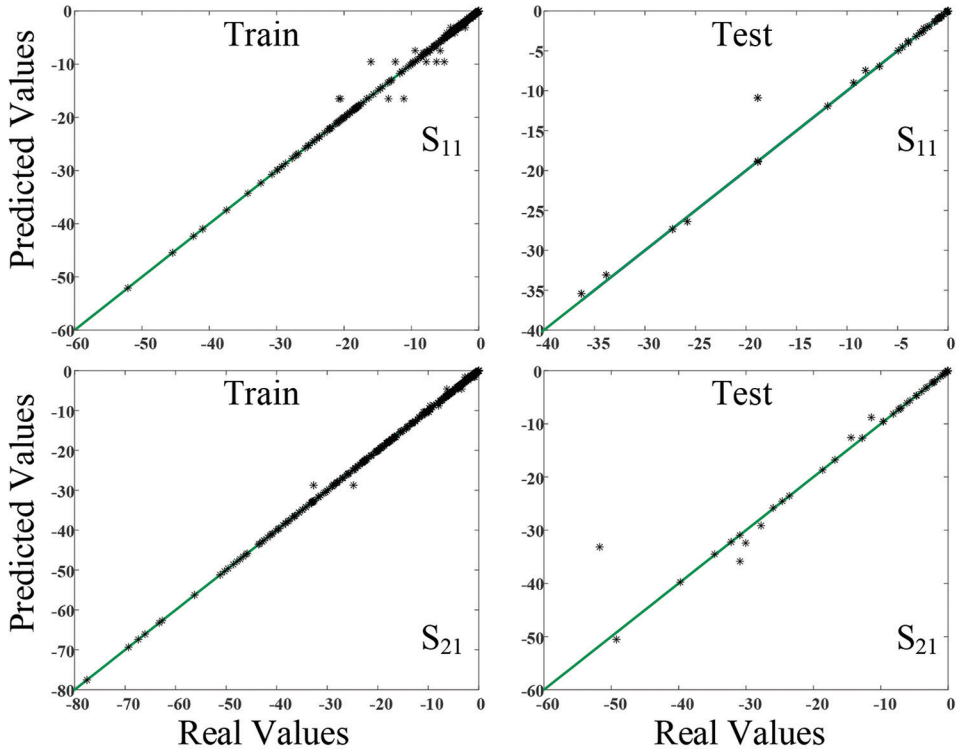

Fig. 11. Real and predicted values for S_{11} and S_{21} parameters in train and test procedures.

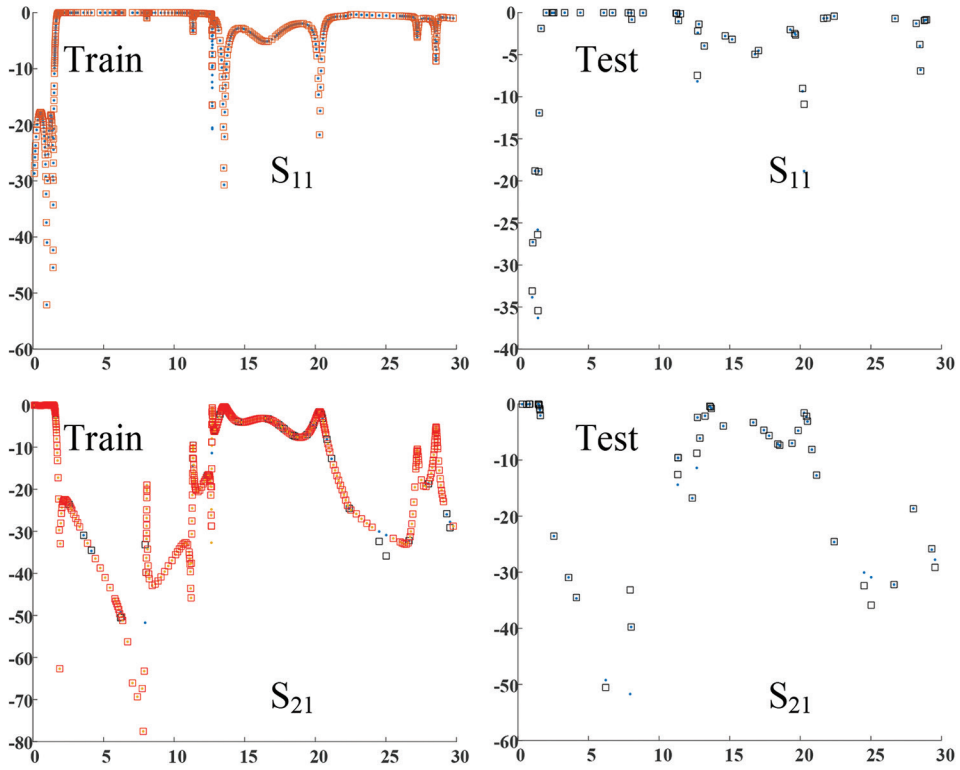

Fig. 12. Real and predicted S-parameters for the proposed device model.

attenuation in this range. The close agreement between the measured and simulated S-parameters highlights the accuracy of the design and the reliability of the fabrication process.

Table I presents a comparative analysis of the performance results of the proposed LPF with several previously filters. The comparison parameters include cutoff frequency, relative stopband width, size, and sharpness of the filter response. The proposed filter exhibits a cutoff frequency of 1.61 GHz and demonstrates a wide RSB. Notably, the proposed design achieves the smallest size among the compared filters.

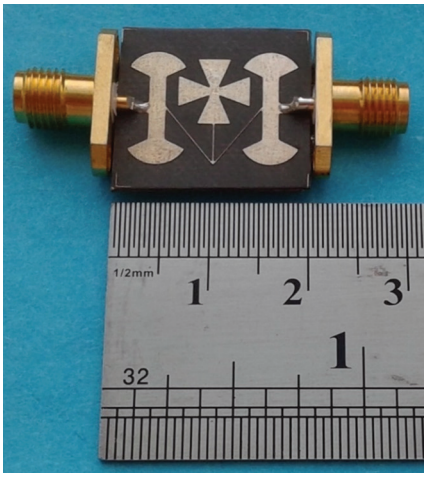

Fig. 13. Fabricated device of the proposed low-pass filter.

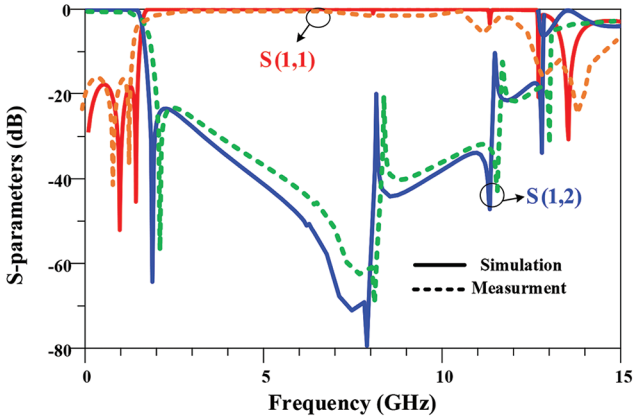

Fig. 14. Measured and simulated S-parameters (S_{11} and S_{21}) of the fabricated low-pass filter with a 1.61 GHz cutoff frequency.

TABLE I
COMPARISON BETWEEN THE PERFORMANCE RESULTS OF THE PROPOSED LPF AND PREVIOUS WORKS

FOM	NCS	RSB	ζ	f_c (GHz)	Ref.
11543	0.0062	1.32	36	1.18	(Wang et al., 2010)
4391	0.0076	1.66	10	3.2	(Ma et al., 2012)
11221	0.0085	1.52	37	1.3	(Ge, Wang and Guo, 2010)
315	0.116	1.46	25	2.95	(Challal et al., 2012)
350	0.009	1.4	37	3.4	(Faraghi, Azarmanesh and Ojaroudi, 2013)
7081	0.006	1.25	22.66	1.67	(Wei et al., 2011)
6009	0.01	1.65	24.28	1	(Wang, Cui and Zhang, 2012)
7815	0.007	1.55	23.53	0.85	(Cui, Wang and Zhang, 2012)
876	0.096	1.22	34.48	2.62	(Mohra, 2011)
4140	0.009	0.68	27.4	2.5	(Yang et al., 2010)
7095	0.02	1.65	43	1.5	(Mandal and Moyra, 2023)
235	0.046	1.32	7.17	2.85	(Ali and Boutejdar, 2017)
612	0.013	1.17	34	3	(Boutejdar, Challal and El Hani, 2018)
31270	0.009	1.49	94.44	1.61	This Work

NCS: Normalized circuit size

Furthermore, the Sharpness (ζ) of the filter response, is the highest in the proposed design. These results highlight the superior performance of the proposed LPF.

The sharpness (ζ) parameter is calculated according to equation (1).

$$\zeta = \frac{\alpha_{max} - \alpha_{min}}{f_s - f_c} \quad (1)$$

Where α_{max} and α_{min} are 60 dB and 3 dB attenuation levels and f_s and f_c are the frequency of the S_{12} parameter at 60 dB, which is equal to 2.21 GHz, and the frequency of the S_{12} parameter at 3 dB frequency which is equal to 1.61 GHz. The sharpness parameter for the proposed filter is 94.44 dB/GHz.

The suppression factor (SF) and related stopband bandwidth (RSB) parameters are calculated according to equations (2) and (3).

$$\text{RSB} = \frac{stopband\ (20\ dB\ attenation\ level)}{stopband\ centre\ frequency} \quad (2)$$

$$\text{SF} = \frac{rejection\ level\ in\ stopband}{10} \quad (3)$$

The designed filter provides a wide stopband from 1.79 GHz to 11.26 GHz, with more than 20dB attenuation level. According to (2) the SF parameter is equal to 2 and according to (3) the RSB parameter is equal to 1.49.

The normalized circuit size is calculated according to (4).

$$\text{NCS} = \frac{physical\ size\ (length \times width)}{\lambda g^2} \quad (4)$$

The figure of merit (FOM) parameter of the proposed filter, is calculated according (5).

$$\text{FOM} = \frac{\zeta \times RSB \times SF}{NCS \times AF} \quad (5)$$

VI. CONCLUSION

A compact microstrip LPF has been designed using a novel windmill-shaped resonator and symmetrical suppressor cells, yielding a wide stopband bandwidth and a sharp transition in the frequency response. The proposed filter achieves a cutoff frequency of 1.61 GHz with a maximum insertion loss of just 0.1 dB within the passband, ensuring efficient signal transmission at desired frequencies. The stopband extends from 1.79 GHz to 11.26 GHz with a minimum attenuation level of 20 dB, significantly reducing out-of-band interference and harmonics over an impressive bandwidth of 9.47 GHz. This expansive stopband performance, combined with a compact size of 13.34 mm × 12.78 mm (0.097λ × 0.093λ), highlights the design's applicability in size-sensitive communication systems. The fabricated prototype was tested, and the experimental results showed excellent alignment with simulated data, confirming the reliability and effectiveness of the design approach. The filter's minimal insertion loss, sharp transition band, and wide stopband address limitations seen in traditional filters, offering a highly efficient, compact, and scalable solution for advanced communication technologies. These characteristics make the proposed filter particularly

suitable for use in modern wireless devices, multi-band communication systems, and ultra-wideband applications where precise frequency control and minimal signal distortion are critical. Overall, the proposed LPF represents a significant advancement in LPF design, providing a robust solution for high-performance communication circuits.

References

Ali, W.A.E., and Boutejdar, A., 2017. Design of low-pass filter using meander inductor and U-form Hi-Lo topology with high compactness factor for L-band applications. *Progress in Electromagnetics Research M*, 55, pp.95-107.

Bavandpour, S.K., Roshani, S., Pirasteh, A., Roshani, S., and Seyedi, H., 2021. A compact low-pass-dual bandpass diplexer with high output ports isolation. *AEU-International Journal of Electronics and Communications*, 135, p.153748.

Boutejdar, A., Challal, M., and El Hani, S., 2018. Design of a new Broad Stop Band (BSB) low-pass filter using compensated capacitor and Π-H-Π DGS resonator for radar applications. *Progress in Electromagnetics Research M*, 73, pp.91-100.

Chakraborty, S., and Verma, A., 2024. Compact high attenuation wide rejection bandwidth 5-pole Butterworth LPF using transmission zeros in GaAs process. *Microelectronics Journal*, 150, p.106263.

Challal, M., Boutejdar, A., Dehmas, M., Azrar, A., and Omar, A., 2012. Compact microstrip low-pass filter design with ultra-wide reject band using a novel quarter-circle DGS shape. *Applied Computational Electromagnetics Society Journal*, 27(10), pp.808-815.

Cui, H., Wang, J., and Zhang, G., 2012. Design of microstrip low-pass filter with compact size and ultra-wide stopband. *Electronics Letters,* 48(14), pp.856-857.

Deng, K., Xue, Q., and Che, W., 2007. Improved compact microstrip resonance cell low-pass filter with wide stopband characteristics. *Electronics Letters*, 43(8), pp.463-464.

Faraghi, A., Azarmanesh, M.N., and Ojaroudi, M., 2013. Small microstrip low-pass filter by using novel defected ground structure for UWB applications. *The Applied Computational Electromagnetics Society Journal*, 28, pp.341-347.

Ge, L., Wang, J., and Guo, Y.X., 2010. Compact microstrip low-pass filter with ultra-wide stopband. *Electronics Letters,* 46(10), pp.689-691.

Hosseini, S.M., and Rezaei, A., 2020. Design of a branch-line microstrip coupler using spirals and step impedance cells for WiMAX applications. *ARO-The Scientific Journal of Koya University,* 8(1), pp.1-4.

Li, L., Li, Z.F., and Wei, Q., 2009. Compact and selective low-pass filter with very wide stopband using tapered compact microstrip resonant cells. *Electronics Letters,* 45(5), pp.267-268.

Lotfi, S., Roshani, S., and Roshani, S., 2020. Design of a miniaturized planar microstrip Wilkinson power divider with harmonic cancellation. *Turkish Journal of Electrical Engineering and Computer Sciences,* 28(6), pp.3126-3136.

Luo, S., Zhu, L., and Sun, S., 2008. Stopband-expanded low-pass filters using microstrip coupled-line hairpin units. *IEEE Microwave and Wireless Components Letters,* 18(8), pp.506-508.

Ma, K., and Yeo, K.S., 2010. New ultra-wide stopband low-pass filter using transformed radial stubs. *IEEE Transactions on Microwave Theory and Techniques*, 59(3), pp.604-611.

Ma, K., Yeo, K.S., and Lim, W.M., 2012. Ultra-wide rejection band low-pass cell. *Electronics Letters*, 48(2), pp.99-100.

Mandal, A., and Moyra, T., 2023. Compact low-pass filter (LPF) with wide harmonic suppression using interdigital capacitor. *Frequenz*, 77(1-2), pp.1-8.

Mandal, M.K., Mondal, P., Sanyal, S., and Chakrabarty, A., 2006. Low insertion-loss, sharp-rejection and compact microstrip low-pass filters. *IEEE Microwave and Wireless Components Letters*, 16(11), pp.600-602.

Meade, R.D., Brommer, K.D., Rappe, A.M., and Joannopoulos, J., 1991. Photonic bound states in periodic dielectric materials. *Physical Review B*, 44(24), p.13772.

Mohammadi, N., Moloudian, G., Roshani, S., Roshani, S., Parandin, F., and Lalbakhsh, A., 2024. A Wilkinson power divider with harmonic suppression through low-pass filter for GSM and LTE applications. *Scientific Reports,* 14(1), p.2429.

Mohra, A.S., 2011. Microstrip low pass filter with wideband rejection using opened circuit stubs and Z-slots defected ground structures. *Microwave and Optical Technology Letters*, 53(4), pp.811-815.

Park, J., Kim, J.P., and Nam, S., 2007. Design of a novel harmonic-suppressed microstrip low-pass filter. *IEEE Microwave and Wireless Components Letters,* 17(6), pp.424-426.

Rezaei, A., and Yahya, S.I., 2022. A new design approach for a compact microstrip diplexer with good passband characteristics. *ARO-The Scientific Journal of Koya University,* 10(2), pp.1-6.

Roshani, S., Dehghani, K., and Roshani, S., 2019. A low-pass filter design using curved and fountain shaped resonators. *Frequenz,* 73(7-8), pp.267-272.

Roshani, S., Koziel, S., Yahya, S.I., Chaudhary, M.A., Ghadi, Y.Y., Roshani,S., and Golunski, L., 2023a. Mutual coupling reduction in antenna arrays using artificial intelligence approach and inverse neural network surrogates. *Sensors*, 23(16), pp.7089.

Roshani, S., Yahya, S.I., Ghadi, Y.Y., Roshani, S., Parandin, F., and Yaghouti, B.D., 2023b. Size reduction and harmonics suppression in microwave power dividers. *ARO-The Scientific Journal of Koya University,* 11(2), pp.122-136.

Ting, S.W., Tam, K.W., and Martins, R., 2006. Miniaturized microstrip low-pass filter with wide stopband using double equilateral U-shaped defected ground structure. *IEEE Microwave and Wireless Components Letters,* 16(5), pp.240-242.

Wang, J., Cui, H., and Zhang, G., 2012. Design of compact microstrip low-pass filter with ultra-wide stopband. *Electronics Letters,* 48(14), pp.854-856.

Wang, J., Xu, L.J., Zhao, S., Guo, Y.X., and Wu, W., 2010. Compact quasi-elliptic microstrip low-pass filter with wide stopband. *Electronics Letters,* 46(20), pp.1384-1385.

Wei, X., Wang, P., Liu, M., and Shi, Y., 2011. Compact wide-stopband low-pass filter using stepped impedance hairpin resonator with radial stubs. *Electronics Letters,* 47(15), pp.862-863.

Yang, M., Xu, J., Zhao, Q., Peng, L., and Li, G., 2010. Compact, broad-stopband low-pass filters using sirs-loaded circular hairpin resonators. *Progress in Electromagnetics Research,* 102, pp.95-106.